Two-Stage Prony-Based Estimation of Fractional Delay and Doppler Shifts in OTFS Modulation

Jitsumatsu, Yutaka
Deptartment of Informatics, Kyushu University

Sun, Liangchen
Department of Information Science and Technology, Kyushu University

出版情報：pp.1-6, 2025-12-12. IEEE
バージョン：

Two-Stage Prony-Based Estimation of Fractional Delay and Doppler Shifts in OTFS Modulation

Yutaka Jitsumatsu
Deptartment of Informatics,
Kyushu University, Japan
jitsumatsu@inf.kyushu-u.ac.jp

Liangchen Sun
Department of Information Science and Technology
Kyushu University, Japan
sun@me.inf.kyushu-u.ac.jp

***Abstract*—Accurate estimation of fractional delay and Doppler shifts in multipath channels is essential for integrated sensing and communication (ISAC) systems operating in high-mobility environments. Such channels exhibit doubly selective fading in both time and frequency. Orthogonal Time Frequency Space (OTFS) modulation provides a simple and robust means for channel compensation under these conditions. However, the presence of fractional delay and Doppler components introduces inter-path interference, which degrades estimation accuracy. In this paper, we propose a two-stage estimation method based on Prony's technique using OTFS pilot signals with M subchannels and N pilot repetitions. In the first stage, Doppler frequencies are estimated by jointly solving M coupled Prony equations, exploiting the periodicity of the pilot signal. In the second stage, delays are estimated by applying the discrete Fourier transform (DFT) and Prony's method to each Doppler component obtained in the first stage. The proposed method can accurately estimate up to $N-1$ delay-Doppler parameters under noiseless conditions. In noisy environments, conventional information criteria such as AIC and BIC yield suboptimal performance; thus, a heuristic model order selection is adopted. Numerical simulations confirm that the proposed method achieves high estimation accuracy, highlighting its potential for future ISAC frameworks.**

***Index Terms*—OTFS, channel estimation, fractional delay Doppler estimation**

I. Introduction

Orthogonal Time Frequency Space (OTFS) modulation [1]–[3] has attracted growing interest as a promising solution for high-mobility communication systems, owing to its robustness against Doppler spread. In addition to communications, OTFS is also regarded as a strong candidate for integrated sensing and communication (ISAC) systems [4]–[6], where radar and communication functionalities are jointly realized within a unified framework.

Accurate estimation of delay and Doppler parameters in multipath channels is critical for both communication and sensing applications. When these parameters align with the integer grid in the delay-Doppler (DD) domain, OTFS enables simple and efficient estimation. However, in practical environments, delays and Doppler shifts often contain fractional components. These cause energy leakage across neighboring DD bins and mutual interference among multipath components, significantly degrading estimation accuracy.

This work was supported in part by JSPS KAKENHI Number JP23K26104 and JP23H00474.

Several methods have been proposed to address this challenge. Gaudio et al. [7] demonstrated the effectiveness of OTFS for joint radar parameter estimation and communication. More recent studies have focused on fractional parameter estimation: Muppaneni et al. [8] proposed a pilot-correlation-based method; Zhang et al. [9] provided a signal-processing-oriented perspective of OTFS for radar sensing; Zacharia and Devi [10] analyzed the estimation performance in ISAC scenarios; and Ranasinghe et al. [11] developed a sequential method for MIMO-OTFS systems. Despite these advancements, many existing methods rely on grid-based approaches or require a large number of pilots, limiting their estimation precision and efficiency, especially in high-SNR regimes.

In this paper, we propose a two-stage estimation method based on Prony's technique for the accurate extraction of fractional delay and Doppler parameters from OTFS pilot signals. Prony's method is known for its high resolution in estimating the frequencies of complex exponentials in low-noise environments. To extend this inherently one-dimensional technique to the two-dimensional DD domain, we introduce three key innovations:

First, we design the pilot signal to be DFT-friendly, ensuring correct interpretation of the frequency component corresponding to $m = -M/2$ when performing the DFT over $m = 0, 1, \dots, M-1$. This correction is essential because fractional Doppler shifts disturb the signal's periodicity.

Second, we reshape the received signal into a two-dimensional matrix indexed by slow and fast time, such that Doppler shifts appear along the slow-time axis. This structure motivates a two-stage approach: Doppler frequencies are estimated first, and the corresponding delay components are extracted after compensating for Doppler-induced effects.

Third, we formulate a novel system of coupled Prony equations that exploits the periodicity of the pilot signal. By jointly solving multiple equations with shared parameters, this formulation enhances estimation robustness and increases the maximum number of resolvable paths compared to the standard Prony method.

We consider a communication system employing OTFS modulation, where frame synchronization is assumed to be already established. Although synchronization is a necessary prerequisite for communication, it falls outside the scope of this study. In addition, given that the channel may vary over time, channel estimation must be updated periodically, typically on a block-by-block basis.

The remainder of this paper is organized as follows: Section II introduces the system model and describes the structure of the transmitted and received signals. Section III presents the proposed two-stage estimation method. Section IV provides simulation results and discusses model order selection using information-theoretic criteria. Section V concludes the paper.

II. Problem Formulation

We use a center-shifted variant of the Dirichlet kernel as the transmitted pilot signal for delay–Doppler estimation. The signal is defined as

$$s(t) = D_M\left(\frac{t}{T}\right) w(t), \tag{1}$$

$$D_M(x) = \sum_{m=-M/2}^{M/2-1} e^{j2\pi m x} = e^{-j\pi x} \cdot \frac{\sin(\pi M x)}{\sin(\pi x)}, \tag{2}$$

where T denotes the duration of a time slot and $w(t)$ is a rectangular window function of duration NT, with N representing the number of pilot repetitions. The construction of the signal is illustrated in Fig. 1. In the frequency domain, $D_M(t/T)$ has line spectrum at $f = m/T$ for $m = -M/2, \dots, M/2-1$.

Note that Eq. (2) defines a periodic signal with period one. This structure offers a key advantage: the reception and delay–Doppler estimation processes can be efficiently performed using the discrete Fourier transform (DFT). The window function $w(t)$ is designed to center the signal and truncate it around its main lobe, thereby suppressing spectral leakage in the frequency domain.

This signal is similar to, but distinct from, the conventional OTFS pilot signal defined in the delay–Doppler (DD) domain as

$$X_{\mathrm{DD}}[k,\ell] = \begin{cases} 1, & k = \ell = 0, \\ 0, & \text{otherwise}, \end{cases} \tag{3}$$

with a detailed comparison provided in Appendix A.

Consider a multipath channel with Doppler shifts. Let P denote the number of propagation paths, which is assumed to be unknown but small relative to the signal space dimension NM, i.e., the channel is *sparse*.

Let $t_{d,\max}$ and $f_{D,\max}$ denote the maximum delay and Doppler shift, respectively. For the p-th path, let α_p, $t_{d,p}$, and $f_{D,p}$ denote the attenuation, delay, and Doppler shift, respectively. We assume that α_p is a complex Gaussian random variable. The time slot duration T is chosen to ensure

$$0 < t_{d,p} < T, \quad -\frac{1}{2T} < f_{D,p} < \frac{1}{2T},$$

which implies

$$t_{d,\max} \le T \le \frac{1}{2 f_{D,\max}}.$$

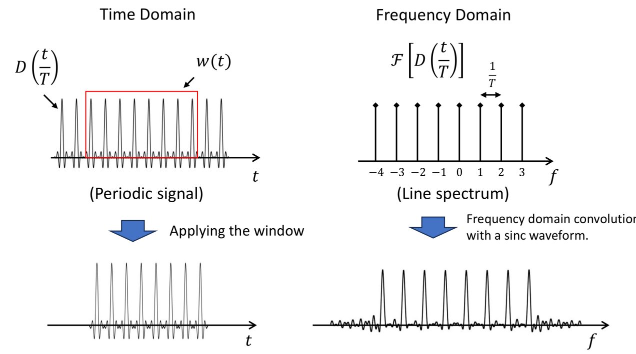

Fig. 1. Construction of the proposed transmitted signal, where $N = M = 8$.

The received signal is given by

$$r(t) = \sum_{p=1}^{P} \alpha_p s(t - t_{d,p}) e^{j2\pi f_{D,p} t} + z(t), \tag{4}$$

where $z(t)$ denotes additive white Gaussian noise (AWGN). The signal is sampled with interval $T_s = T/M$, resulting in

$$r_{\mathrm{TD}}[\ell] = \int r(t) \operatorname{sinc}\left(\frac{t}{T_s} - \ell\right) dt \approx r(\ell T_s), \tag{5}$$

where $\operatorname{sinc}(x) = \frac{\sin(\pi x)}{\pi x}$. This approximation is valid when $f_{D,\max} \ll 1/T_s = M/T$, i.e., when the Doppler spread is much smaller than the signal bandwidth.

Lemma 1: Let $\boldsymbol{R} = (R_{n,\ell})$ be an $N \times M$ matrix defined by

$$R_{n,\ell} = r_{\mathrm{TD}}[nM + \ell],$$

and define $\boldsymbol{E} = (E_{n,p}) \in \mathbb{C}^{N \times P}$ by

$$E_{n,p} = e^{j2\pi f_{D,p} n T}.$$

Let $\boldsymbol{V} = (V_{p,\ell}) \in \mathbb{C}^{P \times M}$ with

$$V_{p,\ell} = \alpha_p D_M\left(\frac{\ell}{M} - \frac{t_{d,p}}{T}\right) e^{j2\pi f_{D,p} \ell T_s}.$$

Then, we have

$$\boldsymbol{R} = \boldsymbol{E}\boldsymbol{V}. \tag{6}$$

The proof is omitted due to space constraints.

This decomposition shows that $\boldsymbol{E}$ depends only on $\{f_{D,p}\}$, making it possible to estimate Doppler frequencies independently of delays. This motivates a two-stage approach: first estimate all $f_{D,p}$, and then estimate the corresponding $t_{d,p}$ and α_p.

In standard OTFS demodulation, the N-point DFT of $R_{n,\ell}$ along n yields the DD-domain signal $Y_{\mathrm{DD}}[k,\ell] = (\boldsymbol{F}_N \boldsymbol{R})_{k,\ell}$, where $(\boldsymbol{F}_N)_{k,n} = e^{-j\frac{2\pi}{N}kn}$. Let

$$t_{d,p} = (\ell_p + \epsilon_{t,p}) T_s, \quad f_{D,p} = \frac{k_p + \epsilon_{f,p}}{NT}, \tag{7}$$

where ℓ_p, k_p are integer parts, and $\epsilon_{t,p}$, $\epsilon_{f,p}$ are the fractional parts.

If $f_{D,p}$ is an integer multiple of $1/(NT)$, then the columns of $\boldsymbol{E}$ are aligned with DFT basis vectors, and $\boldsymbol{F}_N \boldsymbol{E}$ becomes sparse in the Doppler dimension. Thus, $Y_{\mathrm{DD}}[k,\ell]$ is sparse along k, facilitating efficient parameter estimation.

However, in practice, fractional Doppler components cause spectral leakage, reducing sparsity. In such cases, parametric methods like Prony's method are effective for high-resolution estimation.

Assume now that all Doppler frequencies $\{f_{D,p}\}$ are perfectly estimated. Then, the Doppler-induced phase terms in $V_{p,\ell}$ can be removed, yielding the modified signal

$$\widetilde{V}_{p,\ell} = \alpha_p D_M\left(\frac{\ell}{M} - \frac{t_{d,p}}{T}\right). \tag{8}$$

Taking the M-point DFT of $\widetilde{V}_{p,\ell}$ over $\ell = 0, 1, \ldots, M-1$ gives

$$\begin{aligned}&\sum_{\ell=0}^{M-1} \widetilde{V}_{p,\ell}\, e^{-j\frac{2\pi}{M}m\ell}\\ &= \alpha_p \sum_{m'=-M/2}^{M/2-1} \sum_{\ell=0}^{M-1} e^{j2\pi m'\left(\frac{\ell}{M}-\frac{t_{d,p}}{T}\right)} e^{-j\frac{2\pi}{M}m\ell}\\ &= \alpha_p M e^{-j2\pi m'\frac{t_{d,p}}{T}},\end{aligned} \tag{9}$$

where $m' = m$ for $0 \le m < M/2$ and $m' = m - M$ for $M/2 \le m < M$.

This result indicates that $t_{d,p}$ can be estimated by applying Prony's method to the vector $\boldsymbol{V}$.

III. Two-Stage Prony Method

This section presents the proposed Prony-based method, consisting of two estimation stages.

A. Stage 1: Doppler Estimation

The first stage estimates the Doppler shifts. Since $\boldsymbol{R} \in \mathbb{C}^{N\times M}$ has M columns, we apply Prony's method independently to each column. All resulting Prony equations share the same set of solutions, which correspond to the Doppler frequencies. This allows us to formulate M simultaneous equations for estimating the Doppler shifts more robustly. To the best of the authors' knowledge, this approach has not been previously reported in the literature.

Let $\hat{P}$ denote the prescribed number of paths. Its value is determined based on an information criterion. The maximum number of $\hat{P}$ is $N-1$, which is determined by (10) below. Selecting an appropriate value for $\hat{P}$ is one of the most challenging aspects of the proposed method. This issue will be discussed in Section III-D.

For each $\ell = 0, 1, \ldots, M-1$, construct a Toeplitz matrix $T^{(\ell)}$ as

$$T^{(\ell)} = \begin{pmatrix} R_{\hat{P},\ell} & R_{\hat{P}-1,\ell} & \cdots & R_{0,\ell}\\ R_{\hat{P}+1,\ell} & R_{\hat{P},\ell} & \cdots & R_{1,\ell}\\ \vdots & \vdots & & \vdots\\ R_{N-1,\ell} & R_{N-2,\ell} & \cdots & R_{N-\hat{P}-1,\ell}\end{pmatrix}. \tag{10}$$

Then, stack these matrices vertically to form a merged matrix T as

$$T = \begin{bmatrix} T^{(0)}\\ \vdots\\ T^{(M-1)}\end{bmatrix}. \tag{11}$$

The Prony method first determines a vector $\boldsymbol{a} = (a[0], a[1], \ldots, a[\hat{P}])^t$ with $a[0] = 1$ that satisfies $\boldsymbol{Ta} = \boldsymbol{0}$, where $\boldsymbol{0}$ is a zero vector of dimension $M \times (N - \hat{P})$. Let $\boldsymbol{t}_0$ denote the first column of $\boldsymbol{T}$, and let $\widetilde{\boldsymbol{T}}$ denote the matrix obtained by removing the first column from $\boldsymbol{T}$. Then, we obtain

$$\boldsymbol{a}^t = (1, \tilde{\boldsymbol{a}}^t), \tag{12}$$

$$\tilde{\boldsymbol{a}} = -\widetilde{\boldsymbol{T}}^{\dagger}\boldsymbol{t}_0, \tag{13}$$

where $\widetilde{\boldsymbol{T}}^{\dagger}$ is a generalized inverse of $\widetilde{\boldsymbol{T}}$.

Then, find the zeros of the polynomial

$$a[0]x^{\hat{P}} + a[1]x^{\hat{P}-1} + \cdots + a[\hat{P}-1]x + a[\hat{P}] = 0. \tag{14}$$

Denote them by Z_p, for $p = 1, 2, \ldots, \hat{P}$. The estimated Doppler frequency is given by

$$\hat{f}_{D,p} = \frac{\arg(Z_p)}{2\pi T}, \tag{15}$$

where $\arg(Z_p)$ denotes the argument (i.e., phase angle) of the complex number Z_p.

B. Preprocessing before Stage 2

Using the estimated Doppler shifts $\hat{f}_{D,p}$, we reconstruct the matrix $\hat{\boldsymbol{E}}$ as

$$\hat{\boldsymbol{E}} = \left(e^{j2\pi \hat{f}_{D,p} nT}\right)_{n,p}. \tag{16}$$

Then, from (6), the matrix $\boldsymbol{V}$ is estimated as

$$\hat{\boldsymbol{V}} = \arg\min_{\boldsymbol{V}} \left\|\boldsymbol{R} - \hat{\boldsymbol{E}}\boldsymbol{V}\right\|^2 = \hat{\boldsymbol{E}}^{\dagger}\boldsymbol{R}, \tag{17}$$

where $\dagger$ denotes the Moore–Penrose pseudo-inverse. To cancel the Doppler effect in $\hat{\boldsymbol{V}}$, we compute

$$\widetilde{V}_{p,\ell} = \hat{V}_{p,\ell}\, e^{-j2\pi \hat{f}_{D,p}\ell T_s}. \tag{18}$$

Next, we apply the M-point DFT to $\widetilde{V}_{p,\ell}$ for each p to obtain $Y_p[m] = \sum_{\ell=0}^{M-1} \widetilde{V}_{p,\ell}\, W_M^{m\ell}$, where $W_M = e^{-j\frac{2\pi}{M}}$ is the M-th root of unity. If the Doppler shift estimates $\hat{f}_{D,p}$ are perfect and noise is absent, it follows from (9) that

$$Y_p[m] = \alpha_p M\, e^{-j2\pi m t_{d,p}/T} \tag{19}$$

holds for $m = -\frac{M}{2}, -\frac{M}{2}+1, \ldots, \frac{M}{2}-1$.

Remark: Since $Y_p[m]$ is not periodic, the index range for m must be carefully chosen. For periodic signals, the DFT is invariant under circular index shifts (e.g., between $[0, \ldots, M-1]$ and $[-M/2, \ldots, M/2-1]$ when interpreted modulo M). However, this invariance no longer holds for non-periodic complex exponentials. As a result, using the symmetric interval centered around zero is essential for correct interpretation.

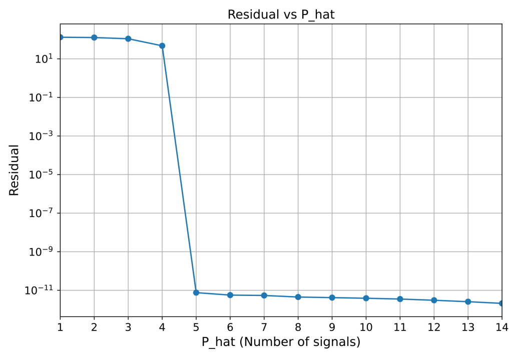

Fig. 2. The residual error of $|\boldsymbol{Ta}\|^2$ against $\hat{P}$. Noiseless case.

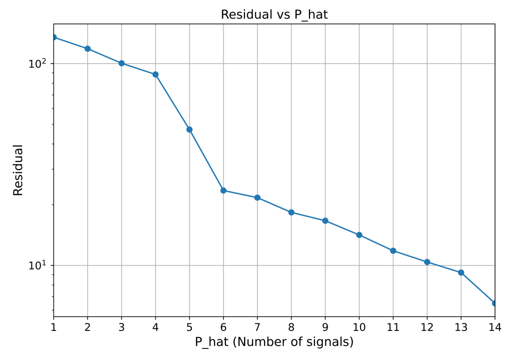

Fig. 3. The residual error of $|\boldsymbol{Ta}\|^2$ against $\hat{P}$, where SNR is 20 dB.

C. Stage 2: Delay Estimation

Let L denote the number of paths sharing the same Doppler shift. The selection of L will be discussed in Section III-D.

For each vector $\boldsymbol{Y}_p = (Y_p[m])_m$, where $p = 1, 2, \ldots, \hat{P}$, we apply Prony's method by constructing a Toeplitz matrix:

$$(\boldsymbol{T}')_{ij} = Y_p\left[L - \tfrac{M}{2} + i - j\right], \tag{20}$$

where $i = 1, \ldots, M - L$ and $j = 1, \ldots, L + 1$.

We then find a nonzero vector $\boldsymbol{a} = (a[0], a[1], \ldots, a[L])^{\mathrm{T}}$ satisfying $\boldsymbol{T}'\boldsymbol{a} = \boldsymbol{0}$, and compute the roots of the polynomial (14) where $\hat{P}$ in (14) is replaced by L. Denote the roots of this polynomial by $Z_{p,\ell}$.

The estimated time delays corresponding to the Doppler shift $\hat{f}_{D,p}$ are then given by

$$\hat{t}_{d,p,\ell} = \frac{\arg Z_{p,\ell}}{2\pi} T, \tag{21}$$

for $\ell = 1, 2, \ldots, L$.

The determination of the estimated number of distinct Doppler shifts, denoted by $\hat{P}$, and the number of delays L associated with each Doppler shift, is of crucial importance.

Figure 2 shows an example of the residual sum of squares (RSS), defined as

$$\mathrm{RSS} = \min_{\|\boldsymbol{a}\|^2=1} \|\boldsymbol{Ta}\|^2, \tag{22}$$

for different values of $\hat{P}$ in the absence of noise. The simulation parameters are set to $N = M = 16$ and $P = 5$. The maximum delay and Doppler shift are $t_{d,\max} = T$ and $f_{d,\max} = 1/(2T)$, respectively. The path gains satisfy $|\alpha_p| = 1$ for all p, and the values of $t_{d,p}$, $f_{D,p}$, and the phase angles of α_p are independently and uniformly distributed. As shown in the figure, when $\hat{P} \geq 5$, the residual error becomes nearly zero.

D. Model order selection

Figure 3 presents the RSS curve for a noisy case with SNR = 20 dB. The RSS decreases monotonically as $\hat{P}$ increases. However, a noticeable change in the slope is observed: the rate of decrease becomes slower for $\hat{P} > P$ when the RSS is plotted on a logarithmic scale.

The choice of an appropriate information criterion is a common issue in hyper-parameter estimation problems. A key challenge in the proposed method is accurately estimating the number of propagation paths, P. To determine the optimal value of $\hat{P}$ at Stage 1, an information-theoretic criterion, such as Akaike's Information Criterion (AIC) or the Bayesian Information Criterion (BIC), should be employed. Specifically, AIC and BIC are defined as

$$\mathrm{AIC} = 2(3\hat{P}) + N \log\left(\frac{\mathrm{RRS}}{N}\right) + \mathrm{const}, \tag{23}$$

$$\mathrm{BIC} = (3\hat{P}) \log N + N \log\left(\frac{\mathrm{RRS}}{N}\right) + \mathrm{const}. \tag{24}$$

Here, $3\hat{P}$ represents the total number of free parameters, assuming each path contributes one complex gain α_p, one delay $t_{d,p}$, and one Doppler frequency $f_{D,p}$. $|\alpha_p|$ was set to one only for drawing Figure 2. For simulation α_p follows a complex Gaussian distribution. Although model selection criteria such as AIC and BIC are fundamental tools for this purpose, they often fail to provide reliable estimates in practice. These criteria tend to either overestimate or underestimate the true value, making it difficult to determine P robustly. Heuristic approaches may therefore be helpful in addressing this issue.

Since AIC and BIC do not provide reliable estimates in our setting, we employed the following heuristic approach instead. Let $\hat{P}$ be a temporary overestimate of the true number of paths P. Stage 1 is performed to obtain Doppler frequency estimates $\hat{f}_{D,p}$. Using these estimates, the preprocessing step before Stage 2 is executed to construct $\tilde{\boldsymbol{V}}$. Let the squared L^2-norm of the p-th row of $\tilde{\boldsymbol{V}}$ be denoted by $\|\boldsymbol{V}_p\|^2$. We discard all rows whose squared L^2-norm is less than 10% of the maximum across all rows.

For delay estimation in Stage 2, we employed AIC and BIC, but found it challenging to determine whether the number of delays is one or greater than one. Therefore, we set $L = 1$ throughout our simulations. This assumption limits the capability of the proposed method when multiple paths share nearly identical Doppler shifts.

Further investigation is needed to determine an appropriate value of L. However, in high SNR scenarios, it is still possible

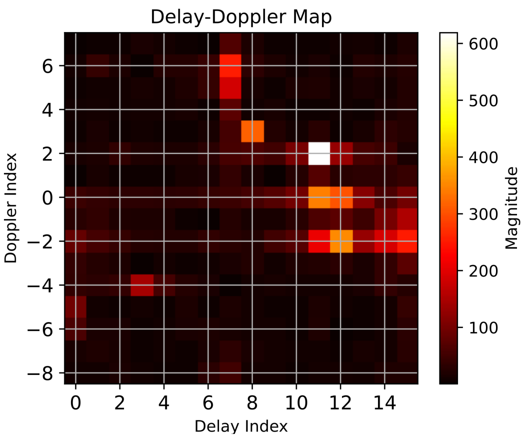

Fig. 4. The absolute value of $Y_{\mathrm{DD}}[k, \ell]$, where $N = M = 16$, $P = 8$, and SNR is 20 dB

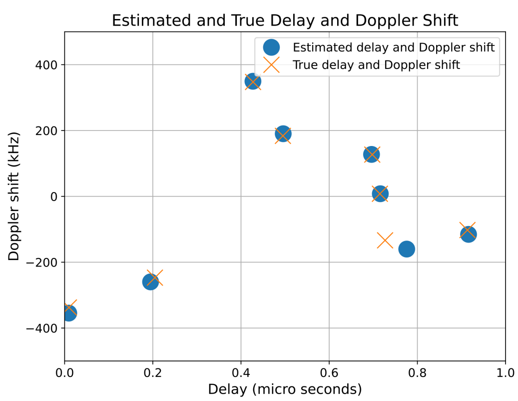

Fig. 5. The true and the estimated delay and Doppler values for the same example shown in Fig. 4

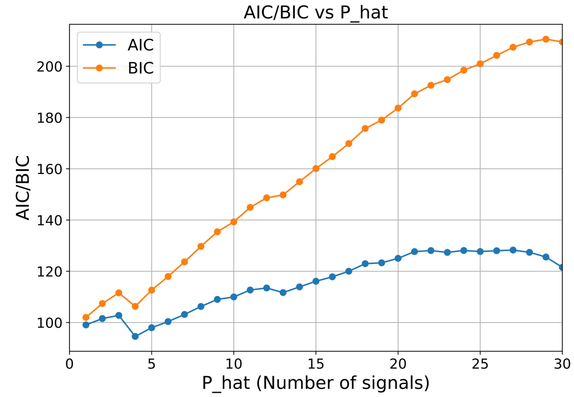

Fig. 6. AIC and BIC vs $\hat{P}$ for $M = N = 32$, $P = 10$ and SNR is 20dB.

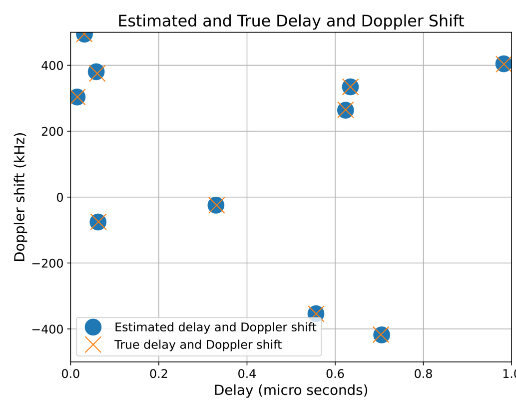

Fig. 7. The true and the estimated delay and Doppler values for $N = M = 32$, $P = 10$, and SNR = 20 dB

to distinguish Doppler frequencies $f_{D,p}$ that are very close to each other. In such cases, the assumption $L = 1$ remains valid.

IV. Simulation Results

Numerical simulation results are reported in this section. Let $T = 1.0 \times 10^{-6}$ seconds. Figure 4 shows the absolute value of the received signal $R_{n,\ell} = r_{\mathrm{TD}}[nM + \ell]$, for $N = M = 16$, $P = 8$, and SNR = 20 dB. Figure 5 presents the true and estimated delay–Doppler values obtained by the proposed method, which shows high accuracy. In this example, AIC was used to estimate $\hat{P}$. From the $Y_{\mathrm{DD}}[k, \ell]$ map, the integer parts of the delay and Doppler shifts can be inferred, though energy leakage may obscure the peaks. Conventional methods refine the fractional parts after coarse estimates [9].

Figure 6 shows the values of AIC and BIC for different values of $\hat{P}$, where $N = M = 32$, $P = 10$, and the SNR is 20 dB. In this example, AIC selects $\hat{P} = 4$, which is significantly smaller than the actual value of P. BIC performs even worse, selecting $\hat{P} = 1$, which leads to a poor estimation result. We observed that AIC generally performs better than BIC, but it still tends to underestimate the number of paths. Therefore, it is preferable to consider values of $\hat{P}$ larger than those suggested by AIC or BIC when selecting candidates for Doppler shifts. To this end, we employed the heuristic approach described in Section III-D, which often yields better estimates than those provided by AIC or BIC. Model order selection is a central topic in machine learning, and it is expected that AI-based approaches will offer improved performance in future implementations.

Figure 7 presents estimation results for $N = M = 32$, $P = 10$, and an SNR of 20 dB. As shown, the proposed method achieves high estimation accuracy when the number of paths is correctly specified.

V. Concluding Remarks

This paper has addressed the problem of delay and Doppler estimation in OTFS modulation, which is essential for communication over doubly selective channels. Accurate estimation enables subsequent channel equalization. Amplitudes can also be estimated in Stage 2, which will be addressed separately.

The proposed two-stage method estimates Doppler shifts first, followed by delays, based on the structure of equation (6). Reversing this order is also possible; in fact, paths with similar Doppler shifts but different delays can be more clearly resolved using this dual approach.

Due to the symmetry of the signal model under Fourier transform, a frequency-domain version of the method can be developed. Running both methods in parallel may improve the estimation of the number of paths and overall accuracy. This will be investigated further.

Accurate delay-Doppler estimation also supports sensing applications, including radar and joint communication-sensing systems. Although a heuristic method was used for model selection, robustness against noise remains a challenge. Integrating learning-based techniques is a promising direction.

In summary, the proposed method contributes to the integration of sensing, AI, and communication via accurate parameter estimation in OTFS systems.

REFERENCES

[1] R. Hadani, S. Rakib, M. Tsatsanis, A. Monk, A. J. Goldsmith, A. F. Molisch, and R. Calderbank, "Orthogonal time frequency space modulation," in *2017 IEEE Wireless Communications and Networking Conference (WCNC)*. IEEE, 2017, pp. 1–6.

[2] S. K. Mohammed, R. Hadani, A. Chockalingam, and R. Calderbank, "OTFS—a mathematical foundation for communication and radar sensing in the delay-Doppler domain," *IEEE BITS the Information Theory Magazine*, vol. 2, no. 2, pp. 36–55, 2022.

[3] ——, "OTFS—predictability in the delay-doppler domain and its value to communication and radar sensing," *IEEE BITS the Information Theory Magazine*, vol. 3, no. 1, pp. 56–75, 2023.

[4] W. Yuan, Z. Wei, S. Li, J. Yuan, and D. W. K. Ng, "Integrated sensing and communication-assisted orthogonal time frequency space transmission for vehicular networks," *IEEE Journal of Selected Topics in Signal Processing*, vol. 15, no. 6, pp. 1515–1528, 2021.

[5] Y. Shi and Y. Huang, "Integrated sensing and communication-assisted user state refinement for OTFS systems," *IEEE Trans. Wireless Comm.*, vol. 23, no. 2, pp. 922–936, 2023.

[6] S. E. Zegrar, H. Haif, and H. Arslan, "OTFS-based ISAC for super-resolution range-velocity profile," *IEEE Trans. Commun.*, 2024.

[7] L. Gaudio, M. Kobayashi, G. Caire, and G. Colavolpe, "On the effectiveness of OTFS for joint radar parameter estimation and communication," *IEEE Trans. Wireless Comm.*, vol. 19, no. 9, pp. 5951–5965, 2020.

[8] S. P. Muppaneni, S. R. Mattu, and A. Chockalingam, "Channel and radar parameter estimation with fractional delay-doppler using OTFS," *IEEE Communications Letters*, vol. 27, no. 5, pp. 1392–1396, 2023.

[9] K. Zhang, W. Yuan, S. Li, F. Liu, F. Gao, P. Fan, and Y. Cai, "Radar sensing via OTFS signaling: A delay doppler signal processing perspective," in *ICC 2023-IEEE Int. Conf. Comm.*, 2023, pp. 6429–6434.

[10] O. Zacharia and M. V. Devi, "Fractional delay and doppler estimation for OTFS based ISAC systems," in *2023 IEEE Wireless Communications and Networking Conference (WCNC)*, 2023, pp. 1–6.

[11] K. R. R. Ranasinghe, H. S. Rou, and G. T. F. de Abreu, "Fast and efficient sequential radar parameter estimation in mimo-otfs systems," in *ICASSP 2024-2024 IEEE Int. Conference on Acoustics, Speech and Signal Processing (ICASSP)*. IEEE, 2024, pp. 8661–8665.

APPENDIX A
COMPARISON BETWEEN THE PROPOSED AND STANDARD OTFS PILOT SIGNALS

In this section, we compare our proposed pilot signal in (1) with the conventional OTFS pilot signal. Our proposed pilot signal can be regarded as a special case of the original OTFS signal definition:

$$s(t) = \sum_{m=-M/2}^{M/2-1} \sum_{n=0}^{N-1} X_{\mathrm{TF}}[n,m]\, g(t-mT)\, e^{jm\frac{2\pi}{T}t}, \quad (25)$$

where $g(t)$ is a rectangular pulse of duration T, and $X_{\mathrm{TF}}[n,m]$ is the time-frequency (TF) domain representation corresponding to the delay-Doppler (DD) domain signal $X_{\mathrm{DD}}[k,\ell]$. The TF-domain signal is obtained via the Symplectic Fourier Transform (SFT) [1] as

$$X_{\mathrm{TF}}[n,m] = \frac{1}{\sqrt{NM}} \sum_{k=0}^{N-1} \sum_{\ell=0}^{M-1} X_{\mathrm{DD}}[k,\ell]\, e^{j2\pi\left(\frac{kn}{N}-\frac{\ell m}{M}\right)}. \quad (26)$$

By substituting the DD-domain pilot in (3) and the SFT expression in (26) into (25), we obtain the pilot signal given in (1). Note that we assume the range of m in (25) is $[-M/2, M/2-1]$.

However, in the current standard OTFS implementation—often referred to as Zak-OTFS—the delay-Doppler (DD) domain signal is directly transformed into a discrete-time domain signal via the discrete Zak transform as

$$x_{\mathrm{TD}}[nM+\ell] = \frac{1}{\sqrt{N}} \sum_{k=0}^{N-1} X_{\mathrm{DD}}[k,\ell]\, e^{j\frac{2\pi}{N}kn}. \quad (27)$$

The transmitted signal is, then, given by

$$s(t) = \sum_{\ell=0}^{M-1} \sum_{n=0}^{N-1} x_{\mathrm{TD}}[nM+\ell]p(t-(nM+\ell)T_s) \quad (28)$$

Using the form of (28), we cannot construct exactly the same signal as (1). However, a kind of dual signal can be constructed by exchanging the time and frequency domains illustated in Figure 1.

Suppose that M is an even number. We can select $p(t)$ as an ideal, frequency-shifted low-pass filter such that its Fourier transform $P(f)$ is given by

$$P(f) = \begin{cases} 1, & \text{if } -\frac{M+1}{2T} < f < \frac{M-1}{2T}, \\ 0, & \text{otherwise.} \end{cases} \quad (29)$$

Taking the inverse Fourier transform yields

$$p(t) = e^{-j\frac{\pi}{T}t} \frac{\sin\left(\frac{M\pi}{T}t\right)}{\pi t}. \quad (30)$$

The spectral center shift is essential in the proposed method. Such a signal is suitable for use in the two-stage Prony method with the reversed estimation order, as discussed in the Concluding Remarks.